



# IJRASET

International Journal For Research in  
Applied Science and Engineering Technology



---

# INTERNATIONAL JOURNAL FOR RESEARCH

IN APPLIED SCIENCE & ENGINEERING TECHNOLOGY

---

**Volume:** 11    **Issue:** VI    **Month of publication:** June 2023

**DOI:** <https://doi.org/10.22214/ijraset.2023.54230>

[www.ijraset.com](http://www.ijraset.com)

Call:  08813907089

E-mail ID: [ijraset@gmail.com](mailto:ijraset@gmail.com)

# Design of Microstrip Patch Antenna for 5G Communications

Boopathi B<sup>1</sup>, Prof. P. Jothilakshmi<sup>2</sup>

Department of Electronics and Communication Engineering, Sri Venkateswara College of Engineering, Chennai

**Abstract:** This project aims to design and implement a low-profile patch antenna for 5G communication application. The resonating frequency has been chosen as 3.5 GHz for 5G application. Rogers RT5880 (lossy) epoxy material with permittivity of 2.2 has been chosen for the substrate material which has fire redundant property. The size of the substrate is 60×60 mm. The proposed antenna is compact Star-Shape radiating patch with defected ground structure, and the feeding technique is used as strip line feed. This proposed Star-Shaped antenna has been designed, analyzed and simulated by CST microwave studio, an electromagnetic simulation software. Antenna parameters like S-Parameter, Antenna Gain, Directivity, Efficiency has been observed and tabulated the results. This proposed Star-Shape antenna is widely used for 5G mobile communication applications.

## I. INTRODUCTION

Modern communication systems require antennas with Narrow bandwidths and smaller dimensions than conventionally possible. Using different antennas to include all communication bands is a straightforward approach, but at the same time, it leads to increasing cost, weight, more surface area for installation, and above all electromagnetic compatibility issues. Thus, there is the need for narrowband width antennas. Microstrip antenna is a good candidate for spiral narrowband antenna design due to its attractive features of low profile, light weight, easy fabrication, and conformability to mounting hosts. A spiral antenna transmits EM waves having a circular polarization. These features highlight the necessity and significance of the design of spiral antennas.

## II. ANTENNA CONFIGURATION AND DESIGN CONCEPTS

The Microstrip Feed Line technique is used to design the log-periodic spiral antenna. A conducting strip is connected directly to the edge of the microstrip patch. The conducting strip is smaller in width as compared to the patch and this kind of feed arrangement has the advantage that the feed can be etched on the same substrate to provide a planar structure.

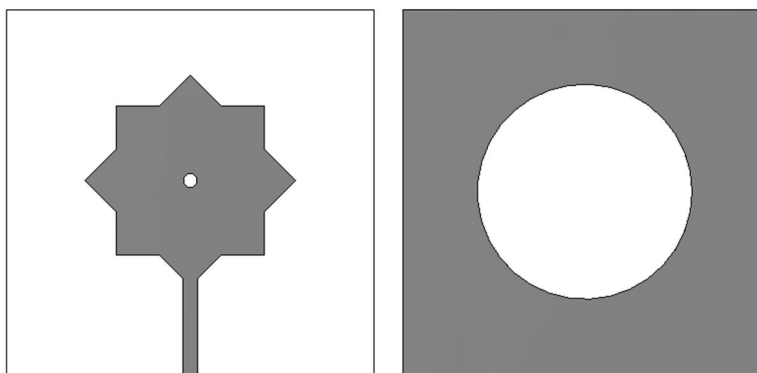


Fig. 1 Proposed Antenna Front and Back View

The structured the proposed low-profile log-periodic antenna is shown in Fig. 1. It is composed of three parts: One is the spiral structured radiating patch, a dielectric substrate and the other is ground plane. To integrate the hybrid spiral structure, microstrip line feed technique is used in this design. The proposed design makes use of log-periodic spiral structures over an elliptical shape center patch. The proposed structure has four log-periodic spiral arms. While the parameter values of Feed Line are Feed length=16.2 mm, and Feed width=2.4 mm. The antenna substrate thickness is  $t = 0.8$  mm. The patch thickness as well as ground plane thickness is 0.035 mm.

To achieve Omni directional radiating pattern, the ground plane had to be cut as circle shape. The ground plane is taken cut out by the circle shape with 35.34 mm diameter.

An SMA connector is used to feed to the feed-line through the ground plane and substrate of the antenna and the antenna performances such as  $|S_{11}|$ , gain and axial ratio when the feed-line is perfectly matched with  $50\Omega$  input impedance.

The substrate between patch and ground plane plays important role in design it decides the bandwidth as well as size of the microstrip antenna. With increase in dielectric constant both the resonant frequency as well as the bandwidth decreases. So, the antenna system becomes narrowband. With increase in thickness of the substrate, the fringing increases which decreases the resonating frequency of the antenna. While parameters like gain, return loss and bandwidth improves significantly. The proposed antenna makes use of Rogers RT Duroid 5880 substrate. RT Duroid 5880 laminates has a low dielectric constant and low dielectric loss, making them well suited for high frequency/broadband applications. Rogers RT Duroid has uniform electrical properties over wide frequency range and has lowest electrical loss for reinforced PTFE material. Rogers RT Duroid is a well-established material and it is easily cut, shared and machined to shape.

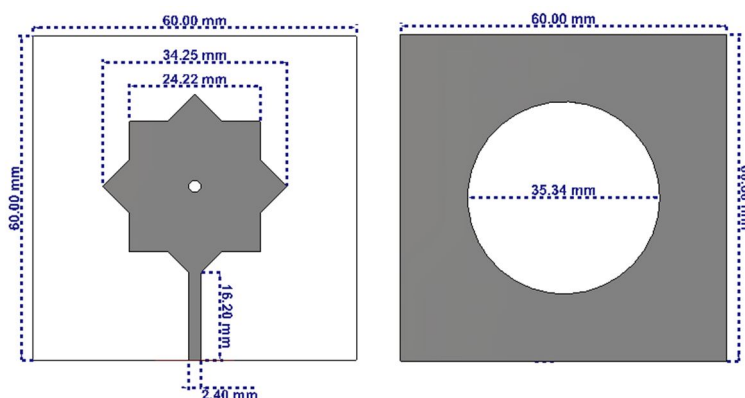


Fig. 2 Proposed Antenna with Dimensions

### III. SIMULATION RESULTS

Simulation enables the use of virtual prototyping. Device performance can be optimized, potential compliance issues identified and mitigated early in the design process, the number of physical prototypes required can be reduced, and the risk of test failures. The proposed design is simulated using CST Microwave Studio Suite. CST stands for Computer Simulation Technology. CST Microwave Studio Suite is a high-performance 3D EM analysis software package for designing, analyzing and optimizing electromagnetic (EM) components and systems. It is widely used in high-frequency problems due to fast, accurate simulations and results generation. It is the software used for the design and calculation of the proposed antenna.

#### A. Return Loss

Return loss is the loss of power in the signal returned or reflected by a discontinuity in a transmission line or optical fiber. This discontinuity can be a mismatch with the terminating load or with a device inserted in the line. Return loss is related to both standing wave ratio (SWR) and reflection coefficient. Reflection coefficient shows what fraction of an incident signal is reflected when a source drives a load. A high return loss is desirable and results in a lower insertion loss. The negative sign is dropped from the return loss value, so a large value for return loss indicates a small reflected signal. The return loss of a load is merely the magnitude of the reflection coefficient expressed in decibels.

The equation for return loss is  $-20 \times \log [\text{mag}(\Gamma)]$ . The return loss of the proposed design is -29.758 dB at a center frequency of 3.5 GHz. Lowest value of return loss which represents the maximum coupling of the antenna. The proposed antenna performs well in return loss results ( $S_{11} > -10\text{dB}$ ).

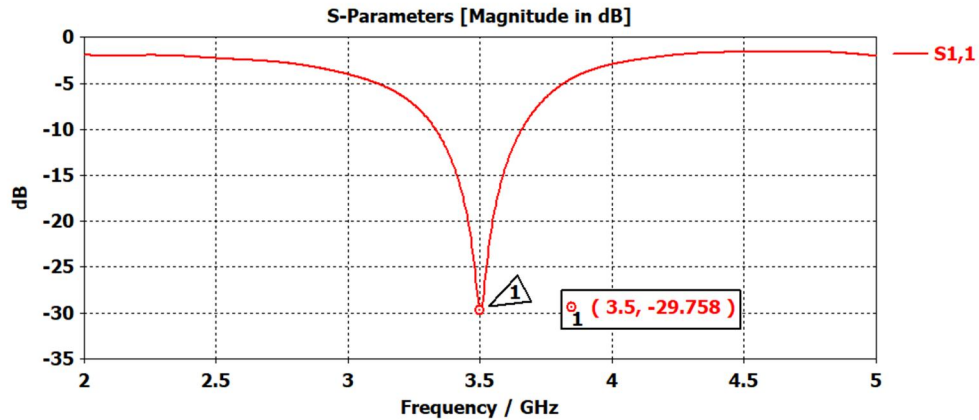


Fig. 3 Simulated Response of S-Parameter

### B. Voltage Standing Wave Ratio (VSWR)

VSWR or sometimes just Standing Wave Ratio (SWR) is a measure of how well matched an antenna is (in terms of impedance) to the transmission line it connects to. If the reflection coefficient is given by  $\Gamma$ , then the VSWR is defined as in equation.

The VSWR is the ratio of the maximum and minimum voltages on the transmission line connected to the antenna, and it follows directly from the reflection coefficient, When the proposed antenna performs well and satisfies the required the conditions as  $VSWR < 2$ .

The VSWR value in the existing microstrip antenna is 1.0672 at a resonant frequency of 3.5 GHz. In this case the feed line has no loss, and matches both the transmitter output impedance and the antenna input impedance, so the maximum power is delivered to the antenna.

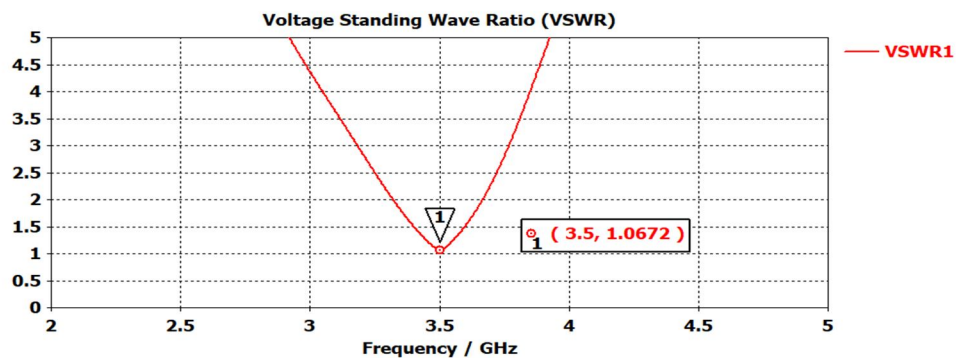


Fig. 4 Simulated Response of VSWR Plot

### C. Farfield Radiation Patterns

The fields radiated by antennas of finite dimensions are spherical waves. Far-field region is defined as that region of the field of an antenna where the angular field distribution is essentially independent of the distance from the antenna. If the antenna has a maximum† overall dimension  $D$ , the far-field region is commonly taken to exist at distances greater than  $2D^2/\lambda$  from the antenna,  $\lambda$  being the free space wavelength. An antenna radiation pattern or antenna pattern is defined as “a mathematical function or a graphical representation of the radiation properties of the antenna as a function of space coordinates.

The radiation pattern is three-dimensional, but usually the measured radiation patterns are a two-dimensional slice of the three-dimensional pattern, in the horizontal or vertical planes. These pattern measurements are presented in either a rectangular or a polar format. In the most common case, antenna radiation patterns are determined in the far-field region. In the far-field region of any antenna the radiated field takes a particularly simple form. The radio signals radiated by an antenna form an electromagnetic field with a definite pattern, depending on the type of antenna used. This radiation pattern shows the antenna’s directional characteristics. A vertical antenna radiates energy equally in all directions a horizontal antenna is mainly bidirectional, and a unidirectional antenna radiates energy in one direction.



**D. Gain**

Gain of an antenna is defined as the ratio of the intensity, in a given direction, to the radiation intensity that would be obtained if the power accepted by the antenna were radiated isotropically, gain of the antenna is closely related to the directivity, it is a measure that takes into account the efficiency of the antenna as well as its directional capabilities. Antenna gain is defined as antenna directivity times a factor representing the radiation efficiency. Antenna gain can also be specified using the total efficiency instead of the radiation efficiency only. This total efficiency is a combination of the radiation efficiency and efficiency linked to the impedance matching of the antenna.

The proposed spiral antenna achieves gain of 4.32 dBi at resonance frequency of 3.5 GHz as shown in fig. Gain is a key performance number which combines the antenna’s directivity and electrical efficiency. The far field gain polar plot of the proposed antenna is shown in Fig. 5. The angular width of main lobe at 3 dB is 68.4 deg.

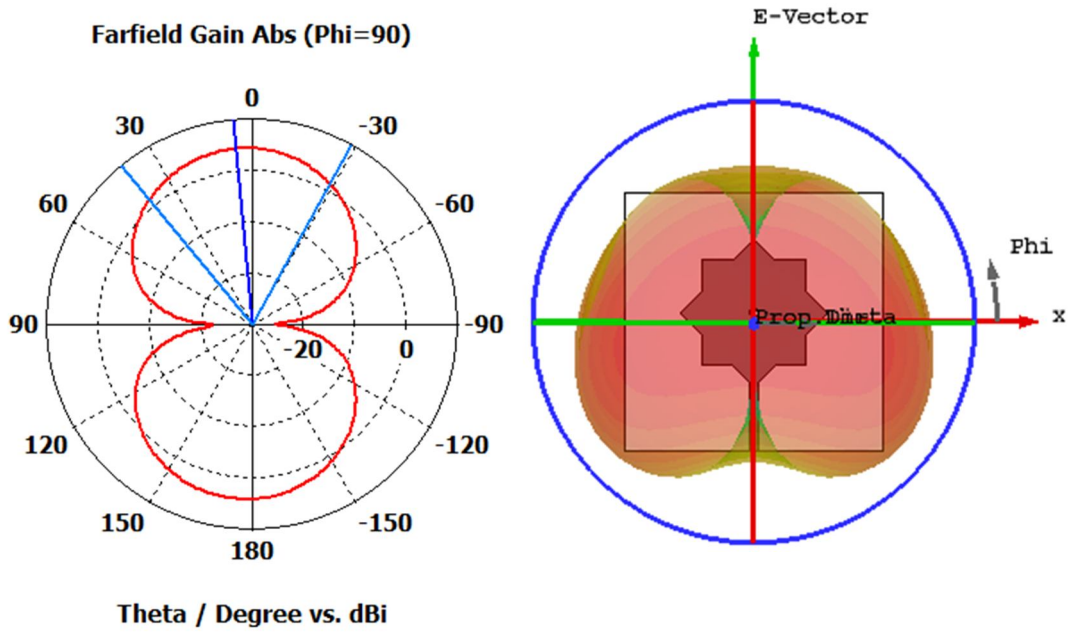


Fig. 5 Far-field Gain Polar and 3D Plot

**E. Directivity**

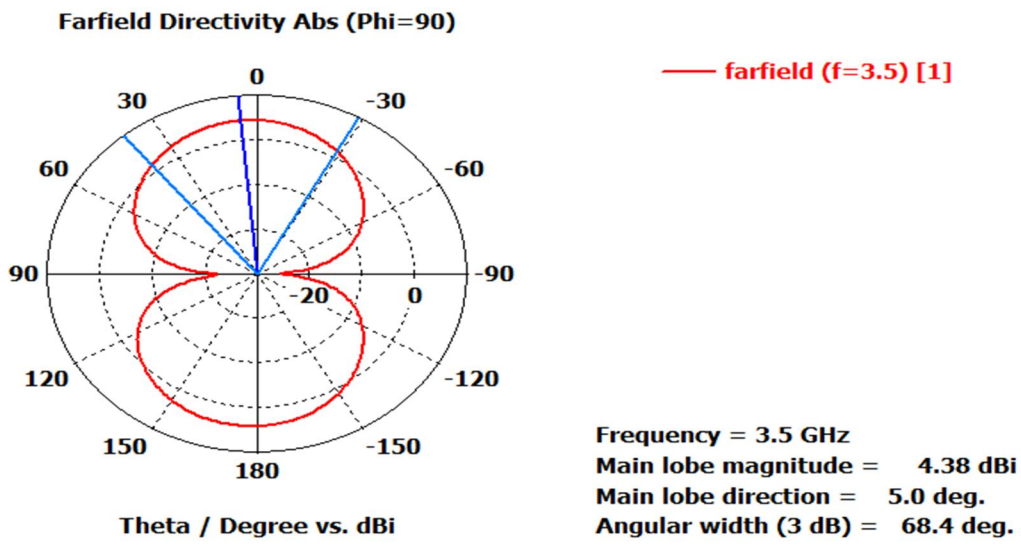


Fig. 6 Far-field Directivity Polar Plot

The ratio of maximum radiation intensity of the subject antenna to the radiation intensity of an isotropic or reference antenna, radiating the same total power is called the directivity. The antenna whose performance is being observed is termed as subject antenna. Its radiation intensity is focused in a particular direction, while it is transmitting or receiving. Directivity is the measure of the concentration of an antenna's radiation pattern in a particular direction. Directivity is expressed in dB. The higher the directivity, the more concentrated or focused is the beam radiated by an antenna.

The directivity of the proposed spiral antenna is shown in Fig. 6. The directivity value achieved by the proposed design is 4.38 dBi. The isotropic antenna is used as a common reference, even though no isotropic antennas exist. The far field directivity polar plot is shown in Fig. 6. A higher directivity also means that the beam will travel further.

**F. E-Field**

The E-field at a point in space is a measure of how strong the force would be on a unit point charge (a small sphere with an electric charge of 1 Coulomb on it). Hence, the units of the E-field are Newtons/Coulomb [N/C]. These units are equivalent to Volts/meter [V/m], which is what the E-field is commonly quoted in (for instance, 10 V/m). The E-field is a vector quantity - this means at every point in space it has a magnitude and a direction. This is the E-field of a plane wave travelling in the +z-direction, and the E-field is linearly polarized and 'points' in the y-direction (k is the wavenumber). The E plane will dictate whether the linear polarization is horizontal or vertical. The amplitude of the wave is A Volts/meter. Fig, shows the Far field Electric Field plot of the proposed antenna.

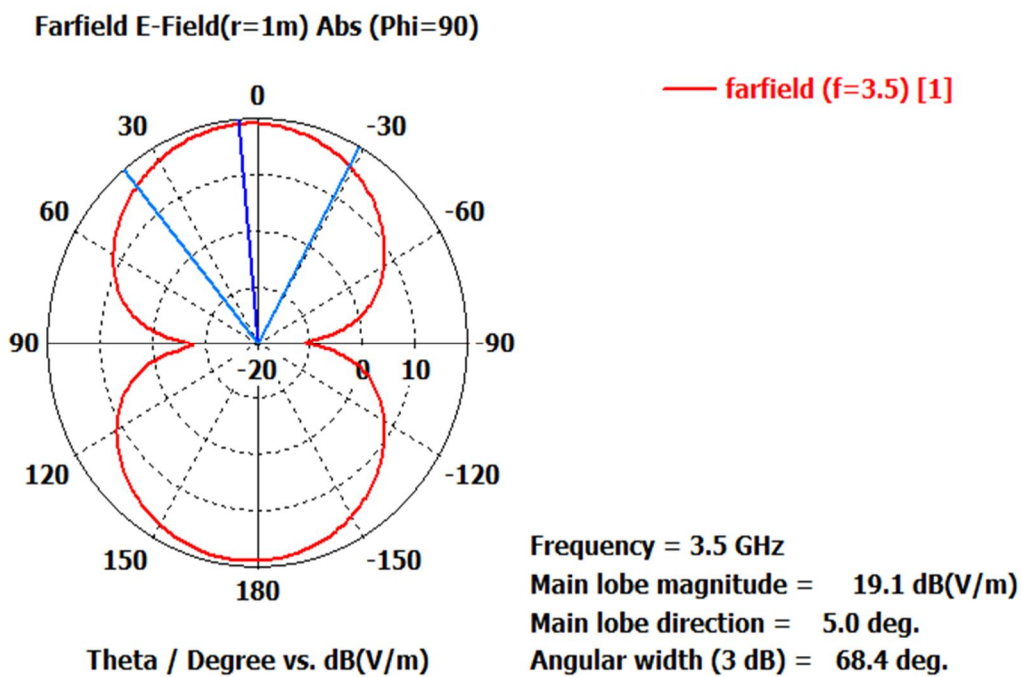


Fig. 7 Far-field Electric Field Plot

**G. H-Field**

The H-field is a vector quantity (has a magnitude and direction) and is measured in Amps/Meter [A/m]. An H-field curls (or wraps) around a wire of moving charge. an H-field can't be defined as a force per unit magnetic charge in the way an E-field can be defined. However, magnetic dipoles do exist (magnets) which have a positive and negative end (or North and South). The magnetic field lines travel away from the North side and terminate on the south side. Fig. 8 shows the Farfield Magnetic Field plot of the proposed antenna. The H-field is orthogonal to the direction of propagation in a plane wave, as well as perpendicular to the E-field. It is the interaction of the E-field with the H-field in space that allows for wave propagation.

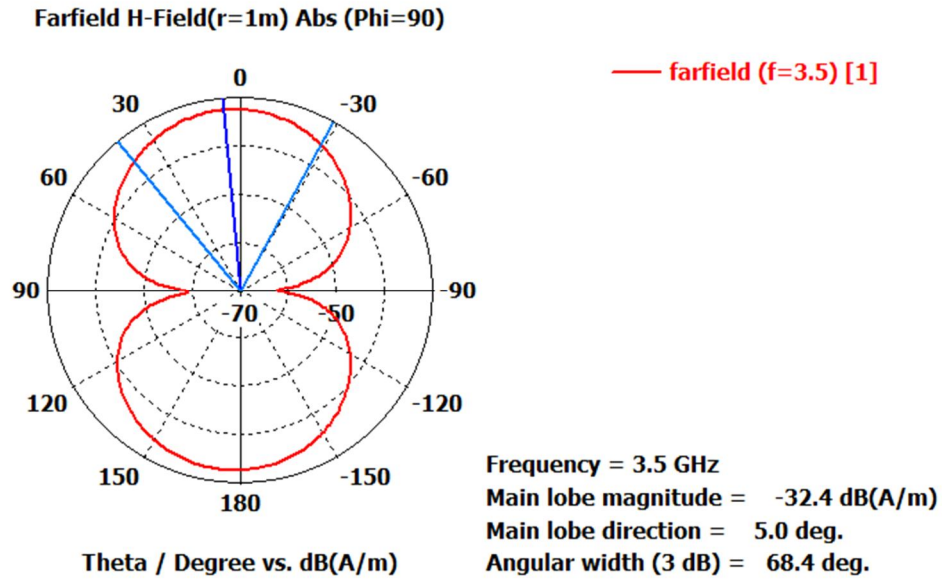


Fig. 8 Far-field Magnetic Field Plot

#### H. Radiation Efficiency

The surface integral of the radiation intensity over the radiation sphere divided by the input power is a measure of the relative power radiated by the antenna, or the antenna efficiency. Material losses in the antenna or reflected power due to poor impedance match reduce the radiated power. The proposed antenna has radiation efficiency of 98.662%.

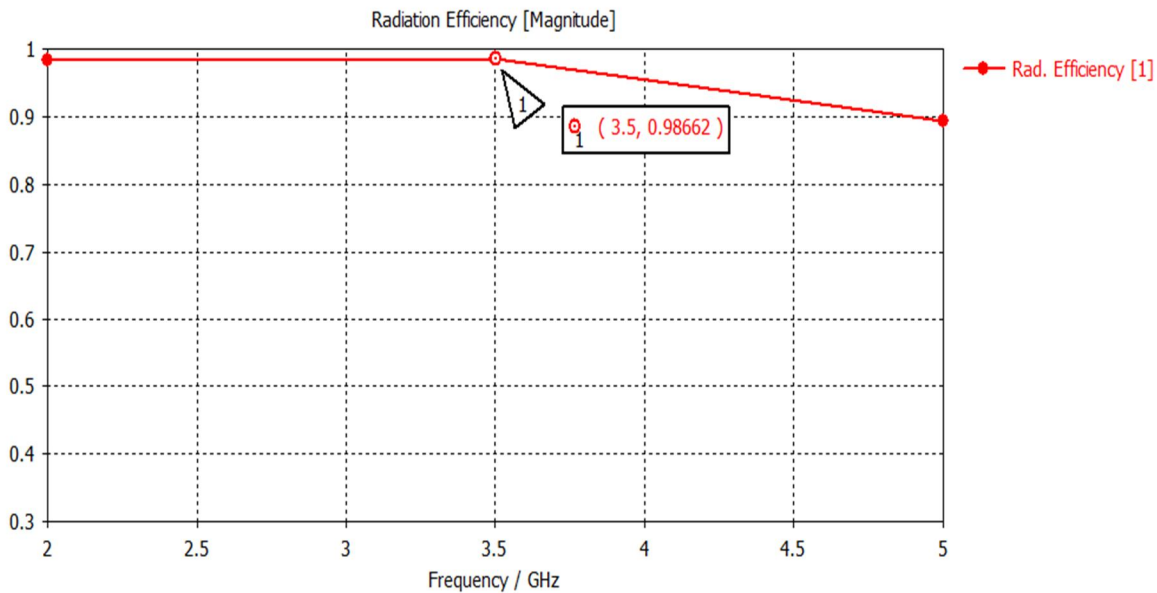


Fig. 9 Radiation Efficiency Plot

#### IV. CONCLUSION

Microstrip antenna has led to many applications in the real world due to its low-profile feature. The star shaped patch antenna has been designed and simulated by using the electromagnetic software CST Microwave Studio Suite. The proposed patch yields desirable results throughout the operating frequency range. The proposed patch antenna achieves a good return loss (-29.758 dB), VSWR (1.0672), good gain (4.32 dBi), good directivity (4.38 dBi) and narrow band-width at 3.5 GHz that determine a long range of operability. Also, it achieves 98.662% radiation efficiency. This proposed microstrip patch antenna design is well suited for fixed mobile service applications.

**REFERENCES**

- [1] X.-H. Ding, W.-W. Yang, W. Qin, and J.-X. Chen, "A broadside shared aperture antenna for (3.5, 26) GHz mobile terminals with steerable beam in millimeter-waveband," *IEEE Trans. Antennas Propag.*, vol. 70, no. 3, pp. 1806–1815, Mar. 2022.
- [2] A.A. Abdulbari, et al., Design compact microstrip patch antenna with T-shaped 5G application, *Bull. Electr. Eng. Info.* 10 (4), pp. 2072–2078, 2021
- [3] G. Gopal, A. Thangakalai, Cross dipole antenna for 4G and sub-6 GHz 5G base station applications, *Appl. Comput. Electromagn. Soc. J.* 35 (1), pp. 16–22, 2020.
- [4] Ishteyaq, M. Shah, M. Issmat, K. Muzaffar, A compact double-band planar printed slot antenna for sub-6 GHz 5G wireless applications, *Int. J. Microwave Wireless Technol.* pp1–9, 2020.
- [5] Valcarce Rial, H. Krauss, J. Hauck, M. Buchholz, F. Aguado Agelet Empirical propagation model for WiMAX at 3.5 GHz in an urban environment *Microwave and optical technology letters* vol. 50 no. 2 pp. 483-487, 2008
- [6] L. Hong, I. J. Wassell, G. E. Athanasiadou, S. Greaves, M. Sellars Wideband tapped delay line channel model at 3.5 GHz for broadband fixed wireless access system as function of subscriber antenna height in suburban environment *Proc. IEEE ICSP'03* pp. 386-390, 2003
- [7] Crosby, V. Abhayawardhana, I. Wassell, M. Brown, M. Sellars Time variability of the foliated fixed wireless access channel at 3.5 GHz *Proc. IEEE VTC'05* pp. 106-110, 2005
- [8] R. P. Torres, B. Cobo, D. Mavares, F. Medina, S. Loredo, M. Engels Measurement and statistical analysis of the temporal variations of a fixed wireless link at 3.5 GHz *Wireless Personal Communications* vol. 37 no. 1–2, pp. 41-59, 2006
- [9] M. Eisenbarth, M. Wegener, R. Scheer, J. Andert, D. S. Buse, F. Klingler, C. Sommer, F. Dressler, P. Reinold, and R. Gries, "Toward smart vehicle-to-everything-connected powertrains: Driving real component test benches in a fully interactive virtual smart city," *IEEE Veh. Technol. Mag.*, vol. 16, no. 1, pp. 75–82, Mar. 2021.
- [10] M. N. Sial, "Stochastic geometry modeling of cellular V2X communication over shared channels," *IEEE Trans. Veh. Technol.*, vol. 68, no. 12, pp. 11873–11887, doi: 10.1109/TVT.2019.2945481, Dec. 2019
- [11] R. Lu, L. Zhang, J. Ni, and Y. Fang, "5G vehicle-to-everything services: Gearing up for security and privacy," *Proc. IEEE*, vol. 108, no. 2, pp. 373–389, doi: 10.1109/JPROC.2019.2948302, Feb. 2020
- [12] B. Feng, J. Chen, S. Yin, C.-Y.-D. Sim, and Z. Zhao, "A tri-polarized antenna with diverse radiation characteristics for 5G and V2X communications," *IEEE Trans. Veh. Technol.*, vol. 69, no. 9, pp. 10115–10126, doi: 10.1109/TVT.2020.3005959, Sep. 2020
- [13] [A. K. Arya, S. Kim, K. Ko, and S. Kim, "Antenna for IoT-based future advanced (5G) railway communication with end-fire radiation," *IEEE Internet Things J.*, vol. 9, no. 9, pp. 7036–7042, doi: 10.1109/JIOT.2021.3113698, May 2022.
- [14] M. Ikram, K. Sultan, M. F. Lateef, and A. S. Alqadami, "A road towards 6G communication—A review of 5G antennas, arrays, and wearable devices," *Electronics*, vol. 11, no. 1, p. 169, 2022.
- [15] M. F. Khajeim, G. Moradi, R. S. Shirazi, S. Zhang, and G. F. Pedersen, "Wideband vertically polarized antenna with endfire radiation for 5G mobile phone applications," *IEEE Antennas Wireless Propag. Lett.*, vol. 19, no. 11, pp. 1948–1952, Nov. 2020.
- [16] Di Paola, S. Zhang, K. Zhao, Z. Ying, T. Bolin, and G. F. Pedersen, "Wideband beam-switchable 28 GHz quasi-Yagi array for mobile devices," *IEEE Trans. Antennas Propag.*, vol. 67, no. 11, pp. 6870–6882, Nov. 2019.
- [17] Park, H. Seong, Y. N. Whang, and W. Hong, "Energy-efficient 5G phased arrays incorporating vertically polarized endfire planar folded slot antenna for mmwave mobile terminals," *IEEE Trans. Antennas Propag.*, vol. 68, no. 1, pp. 230–241, 2019.
- [18] S. Zhang, X. Chen, I. Strytsin, and G. F. Pedersen, "A planar switchable 3-D-coverage phased array antenna and its user effects for 28-GHz mobile terminal applications," *IEEE Trans. Antennas Propag.*, vol. 65, no. 12, pp. 6413–6421, Dec. 2017.
- [19] P. Anjos, D. Schreurs, G. A. E. Vandenbosch, and M. Geurts, "Variable-phase all-pass network synthesis and its application to a 14– 54 GHz multiband continuous-tune phase shifter in silicon," *IEEE Trans. Microw. Theory Techn.*, vol. 68, no. 8, pp. 3480–3496, Aug. 2020
- [20] N. Ojaroudiparchin, M. Shen, S. Zhang, and G. F. Pedersen, "A switchable 3-D-coverage-phased array antenna package for 5G mobile terminals," *IEEE Antennas Wireless Propag. Lett.*, vol. 15, pp. 1747–1750, 2016
- [21] Strytsin, S. Zhang, and G. F. Pedersen, "User impact on phased and switch diversity arrays in 5G mobile terminals," *IEEE Access*, vol. 6, pp. 1616–1623, 2018
- [22] Y. J. Cheng, W. Hong, and K. Wu, "Design of a substrate integrated waveguide modified R-KR lens for millimetre-wave application," *IET Microw., Antennas Propag.*, vol. 4, no. 4, pp. 484–491, Apr. 2010
- [23] J.-W. Lian, Y.-L. Ban, Z. Chen, B. Fu, and C. Xiao, "SIW folded Cassegrain lens for millimeter-wave multibeam application," *IEEE Antennas Wireless Propag. Lett.*, vol. 17, no. 4, pp. 583–586, Apr. 2018





10.22214/IJRASET



45.98



IMPACT FACTOR:  
7.129



IMPACT FACTOR:  
7.429



# INTERNATIONAL JOURNAL FOR RESEARCH

IN APPLIED SCIENCE & ENGINEERING TECHNOLOGY

Call : 08813907089  (24\*7 Support on Whatsapp)